

Light-induced reversible expansion of individual gold nanoplates

Cite as: AIP Advances 7, 105025 (2017); <https://doi.org/10.1063/1.4998703>

Submitted: 02 August 2017 . Accepted: 24 October 2017 . Published Online: 31 October 2017

Jinsheng Lu, Yu Hong, Qiang Li, Yingxin Xu, Wei Fang, and Min Qiu

COLLECTIONS

Paper published as part of the special topic on [Chemical Physics](#), [Energy, Fluids and Plasmas](#), [Materials Science](#) and [Mathematical Physics](#)



View Online



Export Citation



CrossMark

ARTICLES YOU MAY BE INTERESTED IN

[Plasmonic-enhanced targeted nanohealing of metallic nanostructures](#)

Applied Physics Letters **112**, 071108 (2018); <https://doi.org/10.1063/1.5018120>

[Optically controllable nanobreaking of metallic nanowires](#)

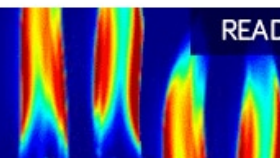
Applied Physics Letters **110**, 081101 (2017); <https://doi.org/10.1063/1.4976947>

[High performance optical absorber based on a plasmonic metamaterial](#)

Applied Physics Letters **96**, 251104 (2010); <https://doi.org/10.1063/1.3442904>

AIP Advances
Fluids and Plasmas Collection

READ NOW



Light-induced reversible expansion of individual gold nanoplates

Jinsheng Lu, Yu Hong, Qiang Li, Yingxin Xu, Wei Fang, and Min Qiu^a
State Key Laboratory of Modern Optical Instrumentation, College of Optical Science and Engineering, Zhejiang University, Hangzhou 310027, China

(Received 2 August 2017; accepted 24 October 2017; published online 31 October 2017)

Light-induced mechanical response of materials has been extensively investigated and widely utilized to convert light energy into mechanical energy directly. The metallic nanomaterials have excellent photothermal properties and show enormous potential in micromechanical actuators, etc. However, the photo-thermo-mechanical properties of individual metallic nanostructures have yet to be well investigated. Here, we experimentally demonstrate a way to realize light-induced reversible expansion of individual gold nanoplates on optical microfibers. The light-induced thermal expansion coefficient is obtained as $21.4 \pm 4.6 \sim 31.5 \pm 4.2 \mu\text{K}^{-1}$ when the light-induced heating temperature of the gold nanoplates is $240 \sim 490 \text{ }^\circ\text{C}$. The photo-thermo-mechanical response time of the gold nanoplates is about $0.3 \pm 0.1 \text{ s}$. This insight into the photo-thermo-mechanical properties of the gold nanoplates could deepen the understanding of the light-induced reversible expansion behavior in nanoscale and pave the way for applications based on this piezoelectric-like response, such as light-driven metallic micromotors. © 2017 Author(s). All article content, except where otherwise noted, is licensed under a Creative Commons Attribution (CC BY) license (<http://creativecommons.org/licenses/by/4.0/>). <https://doi.org/10.1063/1.4998703>

Light, as one kind of ideal clean energy, can be used for controlling objects remotely, instantly, and precisely. Light-absorbing materials can change molecule structures or crystal lattices with light excitation, resulting in changes in their shape or volume. Light can thus be used as a stimuli-driven tool to control the shape or even the motion of objects, and further to convert the light energy into mechanical energy directly.¹ Recently, light-induced mechanical response of various kinds of materials is of significant interest since it provides a new and unexpected way to interact with their environment.² Many works are devoted to polymer materials as they could provide large light-induced deformation.³ With light illumination, the microscopic structural changes of polymer units can be magnified into prominent macroscopic deformations of the whole materials,⁴ including expansion,⁵ contraction,^{6,7} bending,⁸ rotation,¹ climbing⁹ and swimming.² Based on those light-induced deformations, light-driven oscillators,^{10,11} flytraps,¹² springs,¹³ walking robots^{14–16} have been demonstrated. The photo-mechanical properties of carbon nanotubes-based^{17,18} and graphene-based¹⁹ materials have also been studied and the mechanical response to light is mainly due to electrostatic deflections and thermal effects.

On the other hand, metallic nanomaterials show strong absorption of light in visible and near-infrared regions due to their localized surface plasmon resonances.²⁰ The absorbed light is then converted into heat, leading to the increase of lattice size and expansion of the whole metallic structures. Most of works focus on the light-induced shape transformation of metallic nanostructures in colloidal solutions or on a solid substrate under high laser power by measuring the absorption and scattering spectrum or comparing the initial and final shape of the structure with electron microscope.^{21–34} In these cases, the temperature of the nanostructures reaches the melting point of the respective material and the shape transformation is irreversible. The lattice dynamics of metallic nanomaterials after

^aEmail: minqiu@zju.edu.cn

excitation with low-powered femtosecond optical pulses (i.e. in a non-thermal-equilibrium state) are also investigated with the help of X-rays or electron diffraction techniques.^{35–42} However, the photo-thermo-mechanical properties, e.g. the reversible photothermal expansion ability of individual metallic nanostructures in a thermal-equilibrium state, have yet to be well investigated. The characterization of the light-induced reversible expansion in individual nanostructures has been challenging due to the difficulty in simultaneously achieving observation of the individual nanostructures in nanometer resolution and controllable laser irradiation. Understanding the photo-thermo-mechanical properties of individual metallic nanostructures becomes very important as these metallic nanostructures would be the fundamental blocks, e.g., in the construction of light-driven metallic micro/nano actuators.⁴³ The thermal expansion coefficient (TEC) of the individual nanoplates is also yet to be well investigated. Most works dealing with TEC of metallic nanoplates have drawbacks due to their indirect ways of measuring techniques.^{44,45} The nanoplates are on substrate and the TEC measured is that of the nanoplate-substrate combined system. Although some works have taken the TEC of the substrate into consideration,⁴⁵ the values of TEC still differ from each other.^{44,45} Using the microfiber to hold the nanoplate is a better way to eliminate the influence of the substrates and also the nanoplates can expand freely.

Here we experimentally demonstrate a way to realize light-induced reversible expansion of individual gold nanoplates on optical microfibers. The gold nanoplates can expand freely on the microfiber. Relative area expansion of the gold nanoplates under different laser power is measured directly with the help of electron microscope. The photo-thermo-mechanical properties including light-induced thermal expansion coefficient and photo-thermo-mechanical response time of the gold nanoplates are obtained.

The schematic (SEM image) of the photo-thermo-mechanical system in Fig. 1 (Fig. 2 (b)) describes a hexagon gold nanoplates (long side length, 12 μm ; short side length, 8 μm ; thickness, 30 nm) placed and stuck on an optical microfiber (diameter, 2.4 μm) due to strong adhesion arising from the surface related forces (e.g. van der Waals and capillary force).⁴⁶ The photo-thermo-mechanical system is then put into an SEM chamber. A continuous wave laser of wavelength 980 nm is located outside the SEM chamber and connected with the photo-thermo-mechanical system by an optical-through-vacuum connector (see detailed experimental procedures Sec. I and Sec. II in the [supplementary material](#)). In such a way we can achieve observing the gold nanoplates in nanometer resolution and sending laser beam into the SEM chamber simultaneously. After the laser is switched on, the evanescent wave outside the microfiber is absorbed by the gold nanoplate, which, in return, heats the gold nanoplate. The gold nanoplate expands due to the temperature increase. It restores back (i.e. “contract”) to its initial size as the gold nanoplate cools down when the laser is switched off. The gold nanoplate experiences reversible expansion when it is subjected to laser excitation (see [supplementary material](#) video for the process of reversible expansion).

The relative area expansion of the gold nanoplates with respect to the input laser power have been investigated firstly as shown in Fig. 2 (a). For convenience, we choose a red dashed triangle defined by three well-selected points on the gold nanoplates as shown in Fig. 2 (b) to measure the area before (A) and after (A') expansion. The relative area expansion is then calculated as $(A' - A)/A$. The relative area expansion increases with increasing input laser power. As Fig. 2 (c) shows, it takes 0.3 s for the gold nanoplates to expand completely after the CW laser switched on and 0.5 s for the gold nanoplates

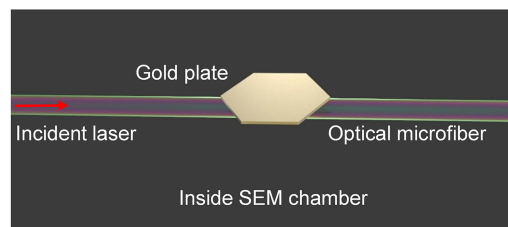


FIG. 1. Schematic of the light-induced reversible thermal expansion of the gold nanoplates. The micron-size gold nanoplate is placed and stuck on the optical microfiber which is inside the scanning electron microscope (SEM) chamber. The gold nanoplate expands reversibly it is excited by a laser (continuous wave laser of wavelength 980 nm).

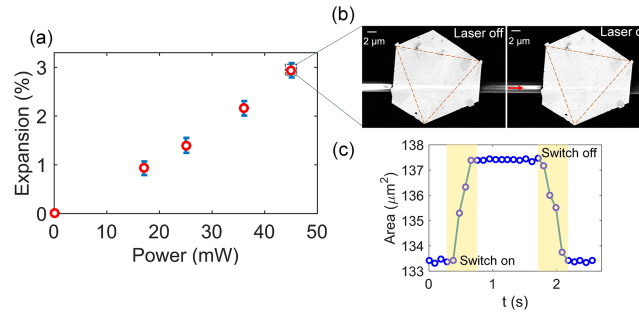


FIG. 2. Experimental results of the light-induced reversible thermal expansion of the gold nanoplates. A hexagonal gold nanoplate (long side length, 12 μm ; short side length, 8 μm ; thickness, 30 nm) is placed on an optical microfiber (diameter, 2.4 μm) guided with continuous wave (wavelength, 980 nm). (a) Relative area expansion of the gold nanoplate with respect to the laser power (for error bar, please see error analysis Sec. IV in the [supplementary material](#)). (b) SEM images of the gold nanoplate on the microfiber and (c) the area reversible expansion of the gold nanoplate when the laser power is 45 mW (see [supplementary material](#) video for the process of reversible expansion). The red dashed triangle defined by three well-selected points on the gold plate in (b) is used to measure the area before and after expansion (see details of area calculation Sec. II 2 in the [supplementary material](#)). The red arrow in (b) indicates the direction of light propagation.

to restore back after the CW laser switched off. Thus the overall response time t_{over} (consisting of the laser switching time t_{laser} , photo-thermo-mechanical response time of gold nanoplates t_{gold} , and the detector exposure time $t_{detector}$ which is determined by the temporal resolution of the electron microscope) can be estimated as 0.4 s ($= (0.3 + 0.5)/2$). The time for laser power to increase from zero to the setting value (to decrease from the setting value to zero) when the laser is switched on (off) is 0.17 s (0.35 s) (see Figure S3 in the [supplementary material](#) for laser switching time). Laser switching time t_{laser} is estimated as 0.26 s ($= (0.17 + 0.35)/2$). The temporal resolution of the electron microscope $t_{detector}$ is 0.1 s. According to the equation: $t_{over} = \sqrt{t_{laser}^2 + t_{gold}^2 + t_{detector}^2}$, the photo-thermo-mechanical response time of the gold nanoplates is determined as 0.3 ± 0.1 s.

To obtain the temperature of the gold nanoplates, three-dimensional (3D) finite-difference time-domain (FDTD) method and COMSOL Multiphysics are combined (see detailed temperature simulations Sec. III in the [supplementary material](#)). The heat source density Q_d induced by light absorption is related to the electric field \mathbf{E} by Ref. 47, $Q_d = \frac{1}{2} \epsilon_0 \omega \text{Im}(\epsilon_r) |\mathbf{E}|^2$ where ϵ_0 and ϵ_r are vacuum permittivity and relative permittivity of gold; ω is the angular frequency of the light (corresponding to the wavelength of 980 nm). The electric field is obtained by FDTD simulations and the temperature distributions is obtained by COMSOL simulations using calculated Q_d as input. It should be noted that the laser power in the microfiber where gold plate is placed is not the same as the input laser power since light attenuates on the way to the gold plate. We use a special way to determine the attenuation. Firstly, we perform an additional experiment to determine the melting point of the gold nanoplates (as shown in Fig. 3 (d)). The gold nanoplate on the silicon substrate heated by the hot stage starts center-melting when the temperature is near 550 $^{\circ}\text{C}$ (see Figure S5 in the [supplementary material](#) for the morphology evolution of the gold nanoplate heated by hot stage). When the temperature is increased to 600 $^{\circ}\text{C}$, most part of the gold nanoplate is melted, which indicates that the melting point of the gold nanoplates can be considered as 600 ± 50 $^{\circ}\text{C}$. Secondly, we increase the input laser power until the gold nanoplates melt noticeably (as shown in Fig. 3 (c)). This happens when the input laser power is 57 mW. In simulations, the laser power in the microfiber where the gold nanoplate is placed should be 8.6 mW when the calculated temperature of the gold nanoplate is 600 $^{\circ}\text{C}$. Thus the attenuation from the input port to the gold plate is estimated as 85% ($= 1 - 8.6/57$). The temperature of the gold nanoplates under other laser powers then can be calculated as shown in Fig. 3 (a).

According to the formula used for the calculation of the thermal expansion coefficient (TEC) α of a thin film:⁴⁸

$$\alpha = \frac{\Delta A/A}{2 \cdot \Delta T},$$

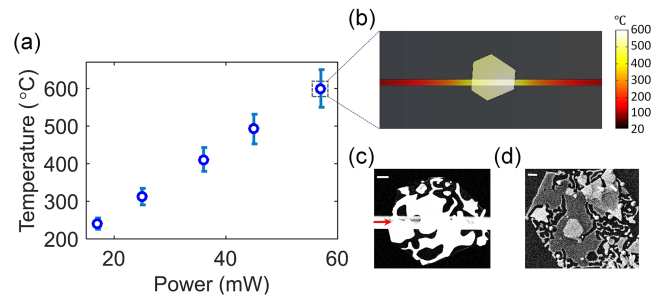


FIG. 3. Simulated temperature of the gold nanoplates. (a) The maximum temperature of the gold nanoplate under different input laser power (for error bar, please see error analysis Sec. IV in the [supplementary material](#)). (b) Temperature distribution of the gold nanoplate-microfiber system and (c) SEM image of the gold nanoplate on the microfiber when the laser power is 57 mW. The gold plate starts to melt heavily when the laser power is gradually increased to 57 mW in (c). The calculated maximum temperature of the gold nanoplate under this laser power is 600 °C. The temperature within the gold nanoplate is almost uniform in (b) (only a difference of a dozen degrees). (d) SEM image of another gold nanoplate placed on the silicon substrate heated by the hot stage when the temperature is increased to 600 °C. Inset scale bars are 2 μm.

where $\Delta A/A$ is the relative area expansion; ΔT is the temperature change of the gold nanoplates, the light-induced thermal expansion coefficient (TEC) is then obtained as $21.4 \pm 4.6 \sim 31.5 \pm 4.2 \mu\text{K}^{-1}$ when the light-induced heating temperature of the gold nanoplates is 240 ~ 490 °C as shown in Fig. 4. TEC of the gold nanoplates increases with temperature, which is similar to the temperature-TEC relationship of copper.⁴⁸ Note that the thermal expansion coefficient is $14.2 \mu\text{K}^{-1}$ for bulk gold.⁴⁹ Our results show that thermal expansion coefficient is much larger for gold nanoplates as compared with that of bulk gold, which is consistent with linear TEC calculated by other methods.^{44,45} This can be explained by the larger surface-to-volume ratio of gold nanoplates. The gold atoms near the surface are exposed to less binding force than those in the volume, and therefore the part near the surface expands more compared to that of volume. Although the specific values of TEC of gold nanoplates measured in an equilibrium state by different groups are different, they are always larger than that of the bulk gold. It is noteworthy to mention that the TEC of ultra-thin (2 ~ 3 nm) gold obtained in a non-equilibrium state under femtosecond laser excitations⁴¹ is $7.6 \mu\text{K}^{-1}$ which is smaller than that of bulk gold. It can be speculated that this anomalous behavior is due to the incomplete expansion (acoustic wave formed) in a non-equilibrium state, whereas we measured it for complete expansion in an equilibrium state.

In conclusion, we have experimentally shown that individual gold nanoplates can expand reversibly on an optical microfiber when the laser is switched on and off. The measured light-induced thermal expansion coefficient is $21.4 \pm 4.6 \sim 31.5 \pm 4.2 \mu\text{K}^{-1}$ when the light-induced heating temperature of the gold nanoplates is 240 ~ 490 °C. The photo-thermo-mechanical response (i.e. reversible expansion) time of the gold nanoplates is about 0.3 ± 0.1 s. This insight into the photo-thermo-mechanical properties of metallic nanostructures would deepen the understanding of the reversible

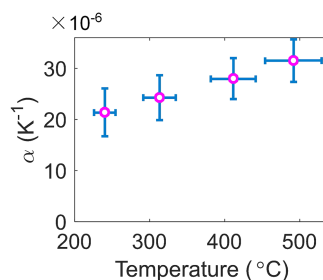


FIG. 4. Light-induced thermal expansion coefficient of the gold nanoplates with increasing temperature. Error bar: the errors resulting from the resolution limitation of the electron microscope (causing error in the expansion area calculations) and the melting range of the gold nanoplates (causing error in the temperature calculations) are taken into account (see error analysis Sec. IV in the [supplementary material](#)).

photo-thermo-mechanical behavior of the metallic structures in nanoscale which is different from that in macroscale. It provides a better method to obtain the thermal expansion coefficient of nanofilms for different materials without adverse effect of substrate. It might pave the way for some interesting applications including light-driven metallic micromechanical actuators, reconfigurable optical components and so on. Typical example includes nanomechanical encoding or switching through reversible thermal expansion.⁵⁰

SUPPLEMENTARY MATERIAL

See [supplementary material](#) for the (I) Microfiber fabrication and micrometer-sized gold plate synthesis, (II) Experimental procedures and expansion measurements, (III) Electromagnetic field simulations and temperature simulations, (IV) Error analysis. (V) Difference between this work and our previous PRL work. See [supplementary material](#) video for the process of light-induced reversible expansion of the gold nanoplates when the input laser power is 45 mW.

ACKNOWLEDGMENTS

We are indebted to Ebba Ahlgren Cederlöf and Filip Klaesson from Royal Institute of Technology (KTH), Sweden, for contributions on the measurements as part of their visiting-student research project. This work was supported by the National Key Research and Development Program of China (No. 2017YFA0205700) and the National Natural Science Foundation of China (Nos. 61425023, 61235007, and 61575177).

- ¹ M. Yamada, M. Kondo, J. Mamiya, Y. Yu, M. Kinoshita, C. J. Barrett, and T. Ikeda, *Angew. Chem. Int. Ed.* **47**, 4986 (2008).
- ² M. Camacho-Lopez, H. Finkelmann, P. Palffy-Muhoray, and M. Shelley, *Nat. Mater.* **3**, 307 (2004).
- ³ T. J. White and D. J. Broer, *Nat. Mater.* **14**, 1087 (2015).
- ⁴ W. Wu, L. M. Yao, T. S. Yang, R. Y. Yin, F. Y. Li, and Y. L. Yu, *J. Am. Chem. Soc.* **133**, 15810 (2011).
- ⁵ O. M. Tanchak and C. J. Barrett, *Macromolecules* **38**, 10566 (2005).
- ⁶ H. Finkelmann, E. Nishikawa, G. G. Pereira, and M. Warner, *Phys. Rev. Lett.* **87**, 015501 (2001).
- ⁷ M. H. Li, P. Keller, B. Li, X. G. Wang, and M. Brunet, *Adv. Mater.* **15**, 569 (2003).
- ⁸ F. T. Cheng, Y. Y. Zhang, R. Y. Yin, and Y. L. Yu, *J. Mater. Chem.* **20**, 4888 (2010).
- ⁹ E. Uchida, R. Azumi, and Y. Norikane, *Nat. Commun.* **6**, 7310 (2015).
- ¹⁰ S. Serak, N. Tabiryran, R. Vergara, T. J. White, R. A. Vaia, and T. J. Bunning, *Soft Matter* **6**, 779 (2010).
- ¹¹ K. Kumar, C. Knie, D. Bleger, M. A. Peletier, H. Friedrich, S. Hecht, D. J. Broer, M. G. Debije, and A. P. Schenning, *Nat. Commun.* **7**, 11975 (2016).
- ¹² O. M. Wani, H. Zeng, and A. Priimagi, *Nat. Commun.* **8**, 15546 (2017).
- ¹³ S. Iamsaard, S. J. Asshoff, B. Matt, T. Kudernac, J. J. L. M. Cornelissen, S. P. Fletcher, and N. Katsonis, *Nat. Chem.* **6**, 229 (2014).
- ¹⁴ F. T. Cheng, R. Y. Yin, Y. Y. Zhang, C. C. Yen, and Y. L. Yu, *Soft Matter* **6**, 3447 (2010).
- ¹⁵ H. Zeng, P. Wasylczyk, C. Parmeggiani, D. Martella, M. Burrese, and D. S. Wiersma, *Adv. Mater.* **27**, 3883 (2015).
- ¹⁶ A. H. Gelebart, D. Jan Mulder, M. Varga, A. Konya, G. Vantomme, E. W. Meijer, R. L. B. Selinger, and D. J. Broer, *Nature* **546**, 632 (2017).
- ¹⁷ Y. Zhang and S. Iijima, *Phys. Rev. Lett.* **82**, 3472 (1999).
- ¹⁸ D. J. Flannigan and A. H. Zewail, *Nano Lett.* **10**, 1892 (2010).
- ¹⁹ J. Mu, C. Hou, H. Wang, Y. Li, Q. Zhang, and M. Zhu, *Sci. Adv.* **1**, e1500533 (2015).
- ²⁰ X. Chen, Y. T. Chen, M. Yan, and M. Qiu, *ACS Nano* **6**, 2550 (2012).
- ²¹ M. Kaempfe, T. Rainer, K. J. Berg, G. Seifert, and H. Graener, *Appl. Phys. Lett.* **74**, 1200 (1999).
- ²² W. Y. Huang, W. Qian, and M. A. El-Sayed, *J. Appl. Phys.* **98**, 114301 (2005).
- ²³ A. Stalmashonak, G. Seifert, and H. Graener, *Opt. Lett.* **32**, 3215 (2007).
- ²⁴ A. A. Unal, A. Stalmashonak, H. Graener, and G. Seifert, *Phys. Rev. B* **80**, 115415 (2009).
- ²⁵ M. Beleites, C. Matyssek, H. H. Blaschek, and G. Seifert, *Nanoscale Res. Lett.* **7**, 315 (2012).
- ²⁶ A. Kuhlicke, S. Schietinger, C. Matyssek, K. Busch, and O. Benson, *Nano Lett.* **13**, 2041 (2013).
- ²⁷ H. H. Liu, O. H. Kwon, J. Tang, and A. H. Zewail, *Nano Lett.* **14**, 946 (2014).
- ²⁸ S. Viarbitskaya, A. Cuche, A. Teulle, J. Sharma, C. Girard, A. Arbouet, and E. Dujardin, *ACS Photonics* **2**, 744 (2015).
- ²⁹ X. Chen, Y. T. Chen, J. Dai, M. Yan, D. Zhao, Q. Li, and M. Qiu, *Nanoscale* **6**, 1756 (2014).
- ³⁰ J. Wang, Y. T. Chen, X. Chen, J. M. Hao, M. Yan, and M. Qiu, *Opt. Express* **19**, 14726 (2011).
- ³¹ K. K. Du, Q. Li, Y. B. Lyu, J. C. Ding, Y. Lu, Z. Y. Cheng, and M. Qiu, *Light: Sci. Appl.* **6**, e16194 (2017).
- ³² L. N. Zhou, J. S. Lu, H. B. Yang, S. Luo, W. Wang, J. Lv, M. Qiu, and Q. Li, *Appl. Phys. Lett.* **110**, 081101 (2017).
- ³³ Q. Li, G. P. Liu, H. B. Yang, W. Wang, S. Luo, S. W. Dai, and M. Qiu, *Appl. Phys. Lett.* **108**, 193101 (2016).
- ³⁴ S. W. Dai, Q. Li, G. P. Liu, H. B. Yang, Y. Q. Yang, D. Zhao, W. Wang, and M. Qiu, *Appl. Phys. Lett.* **108**, 121103 (2016).
- ³⁵ J. Chen, W. K. Chen, J. Tang, and P. M. Rentzepis, *Proc. Natl. Acad. Sci.* **108**, 18887 (2011).

- ³⁶ J. N. Clark, L. Beitra, G. Xiong, A. Higginbotham, D. M. Fritz, H. T. Lemke, D. Zhu, M. Chollet, G. J. Williams, M. Messerschmidt, B. Abbey, R. J. Harder, A. M. Korsunsky, J. S. Wark, and I. K. Robinson, *Science* **341**, 56 (2013).
- ³⁷ A. O. Er, J. Chen, J. Tang, and P. M. Rentzepis, *Appl. Phys. Lett.* **102**, 051915 (2013).
- ³⁸ K. R. Ferguson, M. Bucher, T. Gorkhover, S. Boutet, H. Fukuzawa, J. E. Koglin, Y. Kumagai, A. Lutman, A. Marinelli, M. Messerschmidt, K. Nagaya, J. Turner, K. Ueda, G. J. Williams, P. H. Bucksbaum, and C. Bostedt, *Sci. Adv.* **2**, e1500837 (2016).
- ³⁹ G. F. Mancini, T. Latychevskaia, F. Pennacchio, J. Reguera, F. Stellacci, and F. Carbone, *Nano Lett.* **16**, 2705 (2016).
- ⁴⁰ S. T. Murphy, Y. Giret, S. L. Daraszewicz, A. C. Lim, A. L. Shluger, K. Tanimura, and D. M. Duffy, *Phys. Rev. B* **93**, 104105 (2016).
- ⁴¹ S. Schäfer, W. Liang, and A. H. Zewail, *Chem. Phys. Lett.* **515**, 278 (2011).
- ⁴² J. Hu, T. E. Karam, G. A. Blake, and A. H. Zewail, *Chem. Phys. Lett.* **683**, 258 (2017).
- ⁴³ O. Lehmann and M. Stuke, *Science* **270**, 1644 (1995).
- ⁴⁴ A. T. Pugachev, A. G. Bagmut, N. P. Churakova, and Y. A. Volkov, *JETP Lett.* **38**, 538 (1983).
- ⁴⁵ A. I. Oliva, J. M. Lugo, R. A. Gurubel-Gonzalez, R. J. Centeno, J. E. Corona, and F. Avilés, *Thin Solid Films* **623**, 84 (2017).
- ⁴⁶ J. Lu, H. Yang, L. Zhou, Y. Yang, S. Luo, Q. Li, and M. Qiu, *Phys. Rev. Lett.* **118**, 043601 (2017).
- ⁴⁷ X. Chen, Y. T. Chen, M. Yan, and M. Qiu, *ACS Nano* **6**, 2550 (2012).
- ⁴⁸ J. D. James, J. A. Spittle, S. G. R. Brown, and R. W. Evans, *Meas. Sci. Technol.* **12**, R1 (2001).
- ⁴⁹ D. Lide, *CRC Handbook of Chemistry and Physics* (CRC Press, Florida, 2003), Section 12.
- ⁵⁰ J. O. Lee, K. W. Choi, S. J. Choi, M. H. Kang, M. H. Seo, I. D. Kim, K. Yu, and J. B. Yoon, *ACS Nano* **11**, 7781 (2017).